ACS APPLIED MATERIALS & INTERFACES

Research Article

www.acsami.org

Thermoresponsive Magnetic Nanoparticles for Seawater Desalination

Qipeng Zhao, Ningping Chen, Dieling Zhao, and Xianmao Lu*

Department of Chemical & Biomolecular Engineering, National University of Singapore, 117576 Singapore

Supporting Information

ABSTRACT: Thermoresponsive magnetic nanoparticles (MNPs) as a class of smart materials that respond to a change in temperature may by used as a draw solute to extract water from brackish or seawater by forward osmosis (FO). A distinct advantage is the efficient regeneration of the draw solute and the recovery of water via heat-facilitated magnetic separation. However, the osmotic pressure attained by this type of draw solution is too low to counteract that of seawater. In this work, we have designed a FO draw solution based on multifunctional Fe_3O_4 nanoparticles grafted with copolymer poly(sodium styrene-4-sulfonate)-*co*-poly(*N*-isopropylacrylamide) (PSSS-PNIPAM). The resulting regenerable draw solution shows high osmotic pressure for seawater desalination. This is enabled by three essential functional components integrated within the nanostructure: (i) a Fe_3O_4 core that allows magnetic separation of the nanoparticles from the solvent, (ii) a thermoresponsive polymer, PNIPAM, that enables reversible clustering of the particles for further improved magnetic capturing at a temperature above its low critical solution temperature (LCST), and (iii) a polyelectrolyte, PSSS, that provides an osmotic pressure that is well above that of seawater.

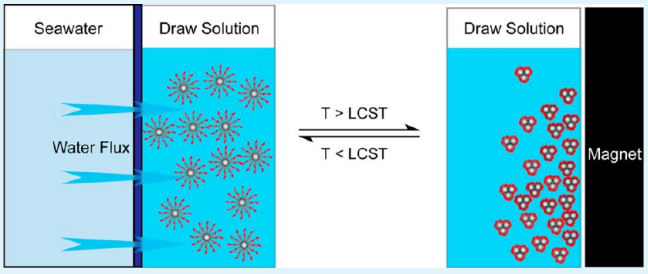

KEYWORDS: *magnetic nanoparticle, thermoresponsive copolymer, polyelectrolyte, forward osmosis, draw solution, seawater desalination*

INTRODUCTION

Freshwater scarcity has become a pressing concern worldwide because of the rapid growth of population and more frequent environmental disruptions. To meet the mounting demand of freshwater, much attention has been directed to wastewater reuse and seawater desalination where membrane technologies play a significant role.[1−4] For seawater desalination, reverse osmosis (RO) has been the dominating membrane process.[5,6] In RO, water is pushed from seawater through a semipermeable membrane to produce freshwater. Because RO process requires a high hydraulic pressure (>55 bar) to overcome the osmotic pressure of seawater, this causes a high electrical energy consumption that has been a major drawback of this process. In recent years, forward osmosis (FO, also known as direct osmosis) has emerged as a promising alternative desalination process.[7−16] In an FO desalination process, a solution with high osmolality (draw solution) is used to draw water from seawater (feed solution) across a semipermeable membrane. A subsequent regeneration process reconcentrates the diluted draw solution and produces freshwater. Because the draw solution has a higher osmolality than the feed solution, the FO process is driven only by the difference in osmotic pressure of the two solutions,eliminating the need for high hydraulic pressure. Therefore, its potential to lower the energy consumption for desalination has been a distinct advantage of FO over other membrane processes.

However, a successful FO desalination process critically relies on the availability of a draw solution that offers both high osmotic pressure and a facile regeneration mechanism.[17,18] Although a high osmotic pressure allows for a high driving force and facilitates the transport of water molecules across the membrane, facile regeneration is essential for the recovery of the draw solute and for the production of freshwater. To date, various draw solutions have been explored for FO desalination. Sugar or inorganic salts have been investigated to desalinate seawater,[19−21] although pure water cannot be obtained because of the poor separation of these solutes from water. Small gas molecules such as ammonia−carbon dioxide have been investigated as FO draw solutes.[22,23] In this case, the recovery of water can be achieved by thermal decomposition. The drawback of this method is that the product water may consist of secondary pollutants. Chemical fertilizers have also been investigated as FO draw solutes.[24] This is an attractive approach because recycling of draw solutes is not necessary (diluted draw solutions containing fertilizer can be directly utilized in fertigation). In addition, organic salts[25,26] and polyelectrolytes[27−29] have been studied as FO draw solutes. However, problems such as high-energy-cost regeneration of the draw solutes or damage of the RO membranes remain to be solved.

Received: September 1, 2013
Accepted: October 17, 2013
Published: October 17, 2013

Scheme 1. Synthesis of MNPs Functionalized with the Thermoresponsive Copolymer PSSS-PNIPAM

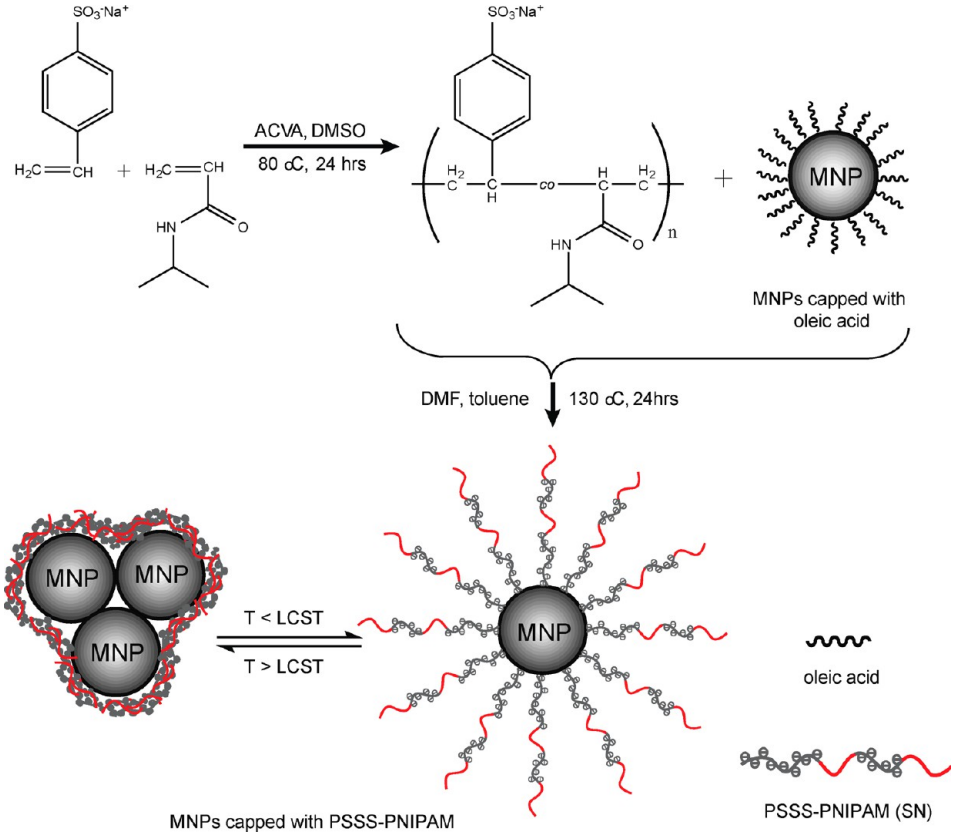

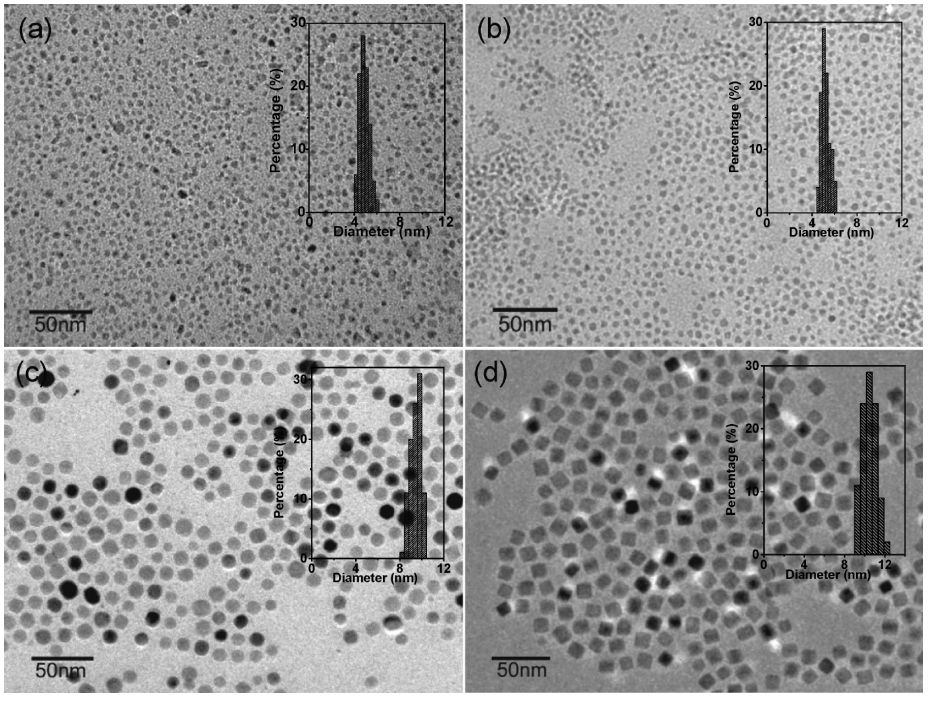

Figure 1. TEM images and size distributions of (a) MNP5, (b) MNP5-15SN, (c) MNP9, and (d) MNP9-15SN.

The rapid progress in nanomaterial research has brought new opportunities for the development of FO draw solutions.[10] For example, when magnetic nanoparticles (MNPs) are used as draw solutes, recovery of water can be achieved by magnetic separation at a relatively low energy expense.[30−37] For MNPs-based draw solutions, the surface modification and the size of the nanoparticles are two crucial factors to achieve higher osmolalities than seawater. This is because the osmolality of a solution is a colligative property that is governed by the number of dissolved solute particles or ions. Therefore, smaller

nanoparticles with high specific surface areas would allow the attachment of a large number of functional groups, whereas functional groups that readily dissociate to give ions would further favor high osmolalities. However, smaller MNPs (<15 nm) are difficult to capture with a magnetic separator.[31] Therefore, there exists a dilemma when magnetic nanoparticles are used as FO draw solutes: ultrasmall MNPs exhibit superior performance over large ones in FO but are unsatisfactory for recovery.[30] One solution for efficient magnetic separation of small MNPs is to achieve reversible aggregation of small nanoparticles into bigger ones. This method could significantly facilitate magnetic capture using a high gradient magnetic separator (HGMS).[31,38,39]

Reversible aggregation of MNPs can be achieved by functionalization with temperature-sensitive polymers such as poly(*N*-isopropylacrylamide) (PNIPAM).[32,40] Heating the solution above its low critical solution temperature (LCST, ~32 °C for PNIPAM) induces clustering of the MNPs because of the shrinkage of the polymer chains.[41,42] Although a few thermoresponsive polymer-based FO draw solutions have been studied previously,[32,43−45] it has been difficult for this class of draw solutions to desalinate seawater because of the limited osmotic pressure provided by thermoresponsive polymers or the lack of a viable regeneration method. Here, we investigate a new design of thermoresponsive MNPs aiming to significantly improve their osmolality for seawater desalination (Scheme 1). In this work, the MNPs are functionalized with a copolymer, poly(sodium styrene-4-sulfonate)-*co*-poly(*N*-isopropylacrylamide) (PSSS-PNIPAM).[46,47] This copolymer integrates two functions: poly(sodium styrene-4-sulfonate) (PSSS) as a polyelectrolyte can dissociate to give a large number of ions in solution and to provide high osmolality, whereas thermoresponsive PNIPAM will facilitate draw-solute regeneration via particle aggregation at temperatures above its LCST. We have found that the MNPs functionalized with PSSS-PNIPAM successfully draw water from seawater. In addition, regeneration of the MNP-based draw solution has been achieved with magnetic separation assisted by mild heating. To the best of our knowledge, this is the first demonstration of seawater desalination using thermoresponsive nanoparticles as a regenerable draw solute.

RESULTS AND DISCUSSION

Characterizations of PSSS-PNIPAM-Functionalized MNPs. Thermoresponsive magnetic nanoparticles functionalized with PSSS-PNIPAM copolymer were synthesized following the procedures described in Scheme 1 (see the Experimental Section for details). The PSSS-PNIPAM copolymers were synthesized in a radical copolymerization reaction.[46] Oleic acid-capped MNPs with two different sizes were prepared on the basis of a modified method reported by Hyeon and co-workers.[48] On the basis of the TEM images shown in Figure 1a,c, the sizes of the MNPs are 4.9 and 9.4 nm (denoted as MNP5 and MNP9), respectively. The MNPs were then functionalized with PSSS-PNIPAM copolymers consisting of 15 wt % PSSS and 85 wt % PNIPAM (15SN) via ligand exchange. The resulting nanoparticles (MNP5-15SN and MNP9-15SN) can be readily dispersed in water. After ligand exchange, the sizes of the nanoparticles increased slightly to 5.2 and 10.5 nm, respectively (Figure 1b,d). To confirm the surface functional groups of the nanoparticles, FTIR spectra were recorded for PSSS, PNIPAM, 15SN, and MNP5-15SN. As shown in Figure 2, characteristic peaks of PNIPAM (1654 and

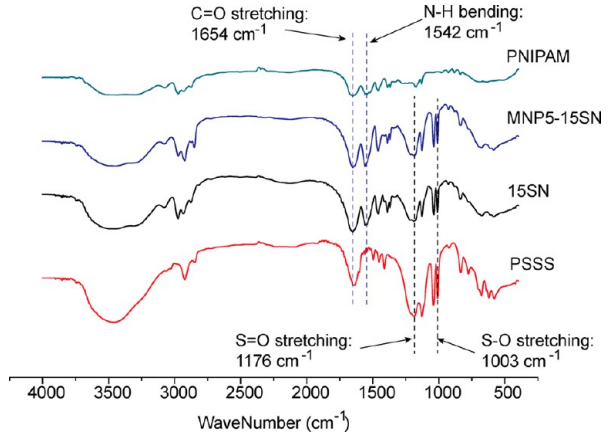

Figure 2. FTIR spectra of PNIPAM, MNP5-15SN, PSSS-PNIPAM, and PSSS.

1542 cm^{-1}, corresponding to C═O stretching and N−H bending, respectively) and PSSS (1176 and 1003 cm^{-1}, corresponding to S═O asymmetric stretching and S−O stretching, respectively) can be found from the spectrum of 15SN. These four peaks are also present in the spectrum of 15SN-capped MNPs, indicating that the copolymer is grafted onto the surface of the nanoparticles.

The amount of functional capping ligands on the surface of the MNPs can significantly affect the performance of the nanoparticles when they are used as a draw solution. From thermal gravimetric analyses (TGA, Figure 3a,b), a continuous weight loss was observed for both MNP5-15SN and MNP9-15SN when the temperature was ramped from 50 to 700 °C. The weight losses for oleic acid-capped MNP5 and MNP9 were 52.3 and 54.7 wt %, respectively, indicating that the amounts of oleic acid attached on the particle surface of MNP5 and MNP9 are similar. For MNP5-15SN and MNP9-15SN, the weight losses were 77.2 and 83.8 wt %, respectively. Because the weight loss of 15SN is 90.7 wt %, the amount of copolymer grafted on particle surface can be estimated by assuming that the oleic acid was completely removed during ligand exchange with 15SN. On the basis of this assumption, the copolymer was estimated to account for 85.1 and 92.4 wt % of the samples for MNP5-15SN and MNP9-15SN, respectively. This relatively high loading of the copolymer is crucial for the MNPs to provide a high enough osmolality when they are dispersed in water.

To examine the thermoresponsive property of the MNPs capped with PSSS-PNIPAM copolymer, we monitored the size change of the nanoparticles at different temperatures using a nanoparticle size analyzer. As shown in Figure 3c, at room temperature, MNP9-15SN shows a hydrodynamic size of ~25 nm. When the temperature was increased from room temperature to 30 °C, the size of the particles started to increase, indicating that the LCST of the copolymer capped on the nanoparticles is around 30 °C. At this temperature, the PNIPAM in the copolymer changed from hydrophilic to hydrophobic, causing decreased steric-repulsion force among the particles. Therefore, the nanoparticles started to aggregate and grow in size. When the temperature was above 32°C, the size of the particles reached ~100 nm. Moreover, sedimentation of the particles was observed quickly after the sample was heated above its LCST, whereas for the sample that was kept at room temperature no sedimentation was observed (Figure 3d). For the MNP5-15SN solution (concentration = 33 wt %), it

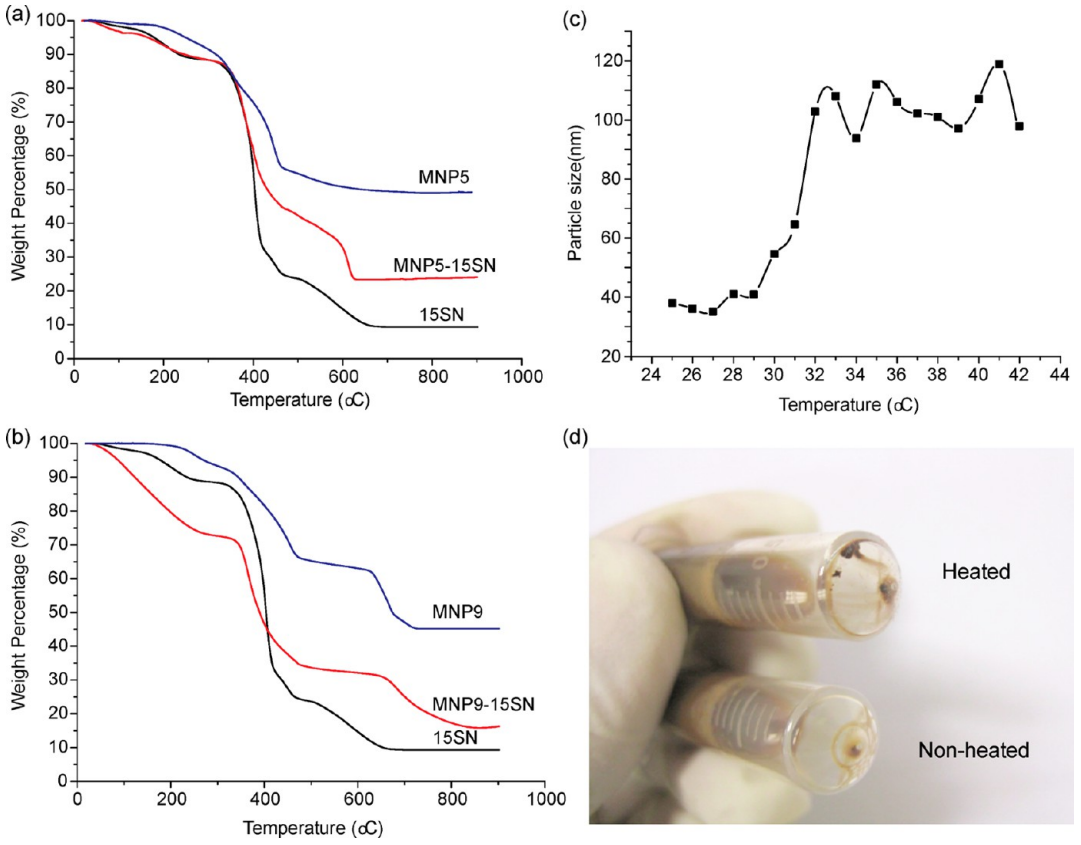

Figure 3. (a, b) TGA analyses of 15SN, MNP5, MNP5-15SN, MNP9, and MNP9-15SN. (c) Hydrodynamic size of the MNPs increased at temperatures above 32 °C. (d) Precipitation of MNPs was found when MNP9-15SN was heated at 70 °C.

was found that 14% of the nanoparticles were precipitated when heated at 70 °C. This temperature-induced aggregation of the MNPs should facilitate further magnetic separation and effective regeneration of the draw solution.

The magnetic property of the MNPs was characterized with vibrating sample magnetometer (VSM) at room temperature. As shown in Figure 4a, the saturated magnetizations for MNP5, MNP9, MNP5-15SN, and MNP9-15SN are 5.38, 12.25, 1.66, and 2.49 emu g^{-1}, respectively. It should be noted that the masses are based on the whole sample, including both iron oxide and the capping ligands. Obviously, the saturated magnetization of the MNPs decreased when grafted with copolymer. With a larger amount of copolymer coated on the nanoparticle surface, the drop in saturated magnetization is larger (79.7% for MNP9 and 69.1% for MNP5). When normalized with the mass of iron oxide, the saturated magnetizations are 11.28, 27.13, 11.12, and 32.72 emu g^{-1} for MNP5, MNP9, MNP5-15SN, and MNP9-15SN, respectively (Figure 4b). The normalized saturated magnetizations of MNP5 and MNP5-15SN are almost the same. However, for MNP9 and MNP9-15SN, the two values differ by 20%. This difference may be attributed to incomplete ligand exchange, resulting in some oleic acid remained on the surface of the nanoparticles. Magnetic capturing of the nanoparticles with high gradient magnetic separator (HGMS) was further examined for MNP5-15SN samples both at room temperature and heated at 70 °C, respectively. In these tests, MNP5-15SN solutions with an initial osmolality of 1178 mOsm kg^{-1} were allowed to pass through the HGMS. The measured osmolalities of the resultant solutions were 833 and 560 mOsm kg^{-1} for the samples without and with heating, respectively, indicating that more MNPs were removed from the solution at temperature above the LCST. This was also confirmed visually on the basis of the digital photos of the samples as shown in Figure 4c. This result confirms that the clustering of nanoparticles at temperatures above the LCST indeed facilitates separation.

Desalination and Cycling Tests. For FO tests, two draw solutions containing MNP5-15SN and MNP9-15SN (33 wt %), respectively, were prepared. The measured osmolalities of the resultant MNP5-15SN and MNP9-15SN solutions are 2250 and 1670 mOsm kg^{-1}, respectively. Assuming an ideal solution, the osmotic pressures of the draw solution (in atm) can be estimated using the van't Hoff equation $\pi = cRT/P_a$, where c is the osmolarity, R is the ideal gas constant (8.314 J K^{-1} mol^{-1}), T is the temperature (298 K), and P_a is the atmosphere pressure (101 325 Pa). The estimated osmotic pressures for MNP9-15SN and MNP5-15SN are 40.8 and 55.0 atm, respectively (Figure 5a). For typical seawater with a salinity of 3.5% (or 1200 mOsm), the osmotic pressure is around 29 atm. It should be noted that because of the relatively high concentration of the solutions, this estimation will not be accurate, but it can be indicative of the relative osmotic pressure of the samples. The lower osmotic pressure of MNP9-15SN compared to MNP5-15SN may be attributed to the large size of the nanoparticles and the incomplete ligand exchange based on the TGA and VSM analyses.

Both MNP5-15SN and MNP9-15SN draw solutions were then evaluated in a FO process with a lab-scale circulating-filtration unit using commercial TFC membrane (Hydration Technologies Inc.). The draw solution was introduced to the active-layer side of the membrane. When DI water was used as feed solution, the water fluxes across the HTI membrane were

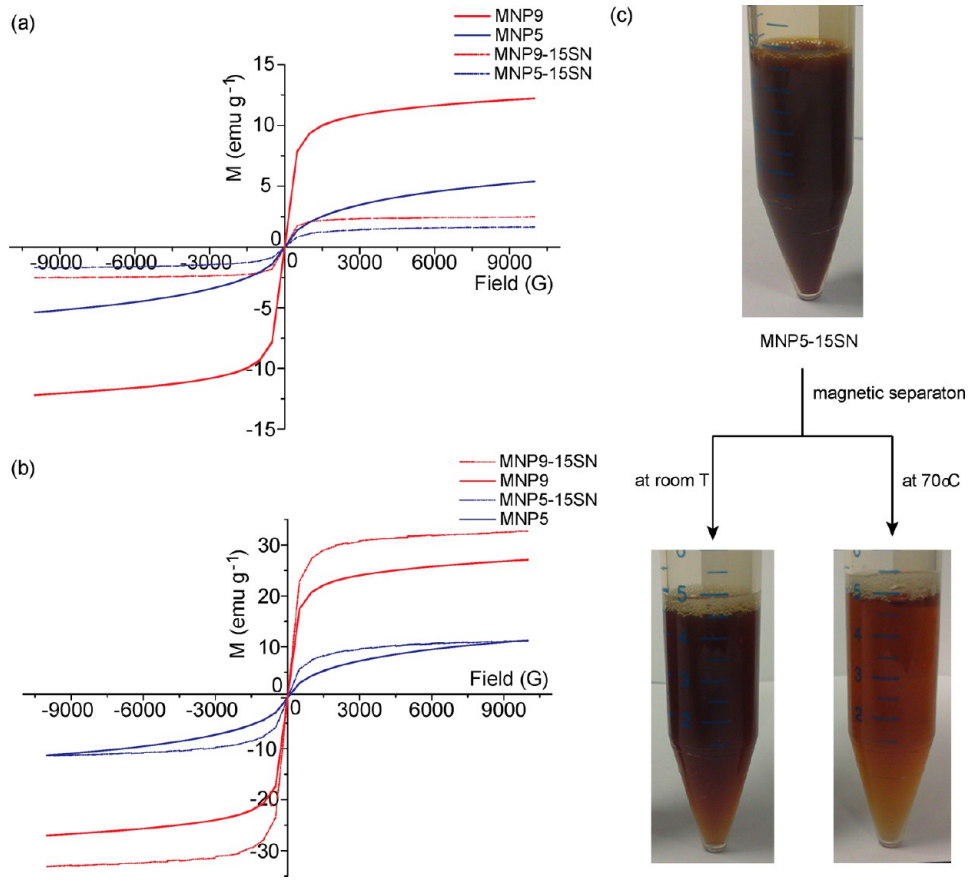

Figure 4. (a) VSM measurements of MNP9, MNP5, MNP9-15SN, and MNP5-15SN. (b) VSM measurements normalized to the weight of nanoparticles. (c) Digital photos showing the effect of magnetic separation for MNP5-15SN at room temperature and heated at 70 °C, respectively.

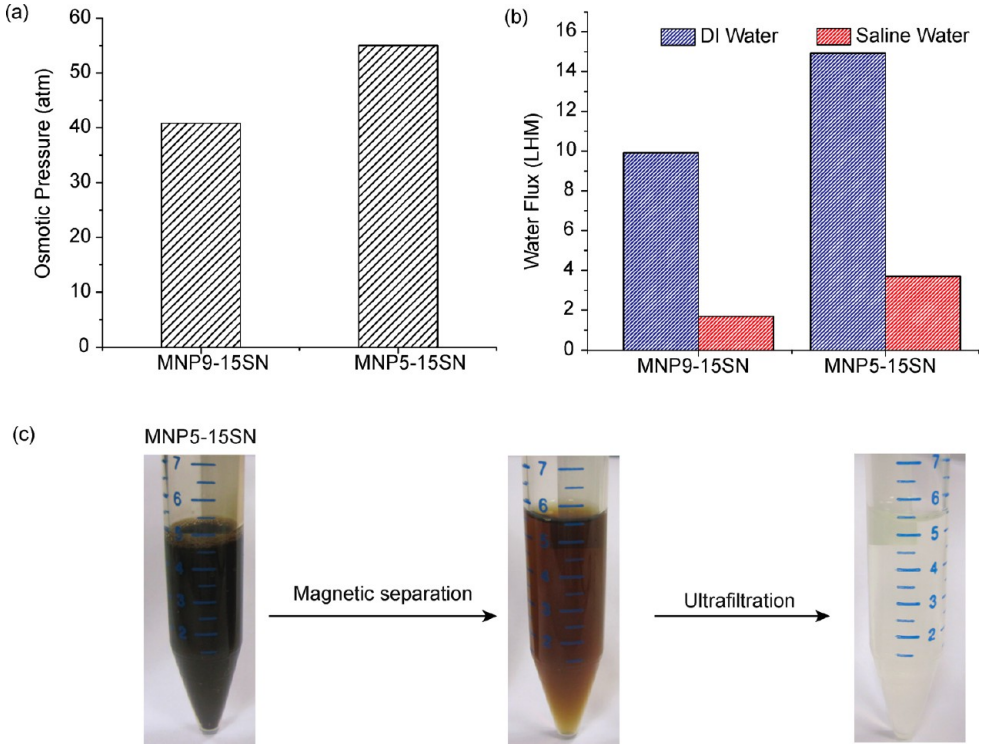

Figure 5. (a) Osmotic pressures and (b) measured water fluxes using DI water and saline water as feed solutions in PRO mode for samples MNP9-15SN and MNP5-15SN (33 wt %), respectively. (c) Separation of MNP5-15SN using HGMS and ultrafiltration.

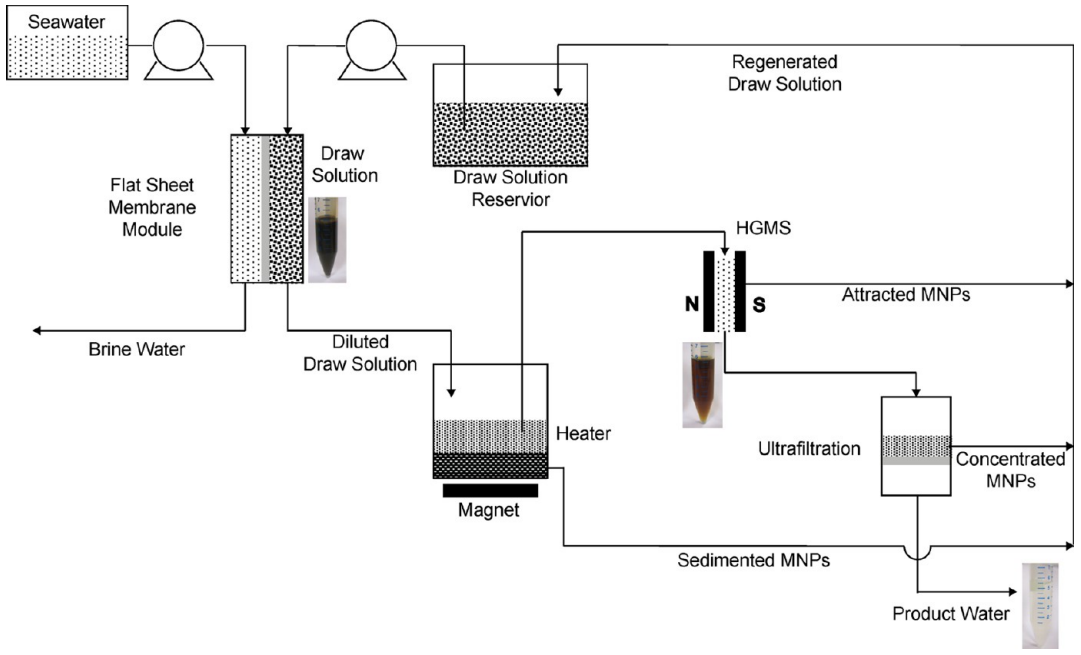

Figure 6. Schematic illustration of the FO process (using MNP-15SN as the draw solution) and the regeneration of the draw solute.

9.9 and 14.9 LMH for MNP9-15SN and MNP5-15SN, respectively. When saline water with an osmolality of 1000 mOsm kg^{-1} was used as the feed solution, the water fluxes decreased to 1.7 and 3.7 LMH for MNP9-15SN and MNP5-15SN, respectively (Figure 5b). Such results are consistent with the osmotic pressures obtained for the two draw solutions, where a larger difference in osmotic pressure between the draw and feed solutions will provide a higher driving force, leading to higher water flux. In addition, such a relationship between the difference in the osmotic pressure and water flux (J_v) can be described as $J_v = \alpha\Delta\pi$, where α is the pure-water permeability coefficient governed by the system and $\Delta\pi$ is the osmotic pressure difference between the bulk draw solution and bulk feed solution.

The PSSS-PNIPAM-functionalized MNPs are responsive to two stimuli: temperature and magnetic field. This property allows a facile approach to recover the MNPs when they are used as a FO draw solute. The regeneration and cycling process of MNP5-15SN for FO desalination is illustrated in Figure 6. The diluted MNP-15SN draw solution after FO was heated above the LCST. (In an industrial process, the required thermal energy for this mild heating can be provided by waste heat from plants[10] or solar heating[49] to minimize energy cost.) Some MNPs aggregated and formed precipitate. The precipitated MNPs were then recycled into the draw solution. The remaining nanoparticles in solution proceeded to the HGMS, where the MNPs were captured by magnetic field. Because it is difficult to remove completely the MNPs with HGMS, the solution was further processed with ultrafiltration to give product water, whereas the MNPs were recycled back to the draw solution. It should be noted that this process was performed in separated steps because of the small scale of the test in this work. Because the MNP5-15SN solution showed a higher osmolality than that of MNP9-15SN, it was selected to demonstrate the FO desalination followed by regeneration process for multiple cycles. Figure 7 shows the water flux of each cycle when the FO was performed with three different feed solutions: DI water, saline water (osmolality = 1000 mOsm kg^{-1}), and simulated seawater (osmolality = 1200 mOsm kg^{-1}), respectively. For the first cycle, the water fluxes corresponding to the feed solutions of DI water, saline water, and seawater were 14.9, 3.7, and 2.7 LMH, respectively. After each cycle, there was a slight drop (<10%) of the water flux. This is mainly caused by the loss of MNPs during the regeneration process. After five cycles, a water flux higher than 2 LMH was still attained when seawater was used as the feed solution. Although further improvement in water flux is necessary for this process to be economically viable, these results indicate that thermoresponsive MNPs functionalized with PSSS-PNIPAM are promising FO draw solutes for seawater desalination.

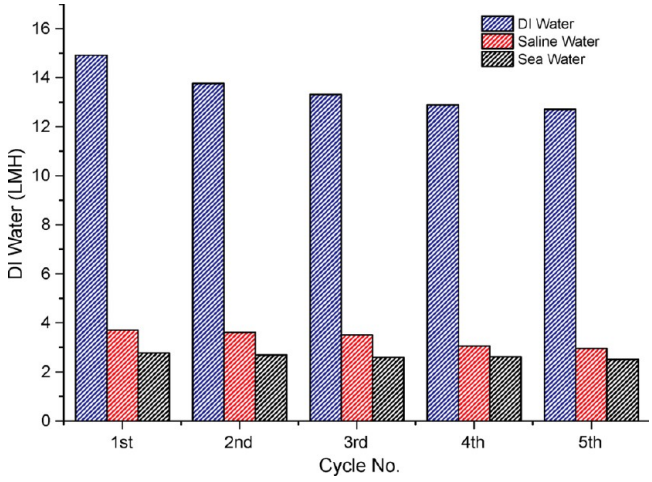

Figure 7. Water fluxes for the MNP5-15SN draw solution (33 wt %) after each cycle using DI water, saline water, and seawater as feed solutions.

CONCLUSIONS

Magnetic nanoparticles functionalized with a thermoresponsive copolymer PSSS-PNIPAM were successfully synthesized and

employed as a draw solute for seawater desalination with a demonstrated regeneration process. This was made possible by three essential functions specifically designed for this nanostructure: (i) the Fe_3O_4 core that allows magnetic separation of the draw solute from water, (ii) the thermoresponsive PNIPAM that enables reversible clustering of the particles to improve magnetic capture when the temperature is above its LCST, and (iii) the polyelectrolyte PSSS that provides an osmotic pressure high enough to counteract that of seawater. When used as draw solution in a FO process, the MNPs-functionalized PSSS-PNIPAM successfully extracted water from seawater and achieved water fluxes larger than 2 LMH. Subsequent magnetic separation of the MNPs assisted by mild heating together with an ultrafiltration step led to regenerated draw solution and freshwater. The results obtained in this work demonstrate that multifunctional magnetic nanoparticles are promising draw solutes in FO processes for seawater desalination. In practical processes, the mild heating may be provided by waste heat from a chemical plant or solar thermal energy to minimize the consumption of high-quality electrical energy. However, it should be noted that further experimental investigation and thermodynamic analysis are necessary to compare the energy required for the regeneration of the thermoresponsive magnetic nanoparticles with that of other FO draw solutes or with the energy consumption in an RO process.

EXPERIMENTAL SECTION

Preparation of Hydrophilic Thermoresponsive Magnetic Nanoparticles. *Materials.* All chemicals and solvents, including iron(III) chloride hexahydrate ($FeCl_3{\cdot}6H_2O$, Sigma-Aldrich, ≥98%), sodium oleate (Sigma, ≥82%), oleic acid (Fluka), oleyl alcohol (Aldrich, 85%), *N*-isopropylacrylamide (NIPAM, Aldrich, 97%), sodium styrene-4-sulfonate (SSS, Aldrich, ≥90%), 4,4′-azobis(4-cyanovaleric acid) (ACVA, Aldrich, ≥98.0%), sodium chloride (Sigma-Aldrich, ≥99%), ethanol (Fisher, HPLC grade), *n*-hexane (Fisher, ACS grade), 1-octadecene (Aldrich, 90%), dimethyl sulfoxide (DMSO, Fisher, AR grade), toluene (Fisher, AR grade), and *N*,*N*-dimethylformamide (DMF, Fisher, HPLC grade), were used as received. Deionized (DI) water (18 MΩ cm) was produced with a Milli-Q system (Millipore).

Synthesis of Iron Oxide Magnetic Nanoparticles (MNPs). The synthesis of iron oxide magnetic nanoparticles functionalized with oleic acid was based on a reported method with some changes.[48,50] First, the MNP precursor iron−oleate complex was synthesized by dissolving 27 g of $FeCl_3{\cdot}6H_2O$ and 111.2 g of sodium oleate in a mixture of solvents containing 200 mL of ethanol, 150 mL of DI water, and 350 mL of hexane. The resulting solution was heated at 70 °C for 4 h. After the reaction was completed, a separatory funnel was used to separate the upper organic layer containing the iron−oleate complex. The iron−oleate complex was then washed with DI water three times. After washing, the iron−oleate complex was stored in solid form by evaporating the hexane.

For the preparation of 9 nm iron oxide nanoparticles, 9 g of iron−oleate complex and 1.43 g of oleic acid were completely dissolved into 50 g of 1-octadecene at room temperature with the assistance of sonication. The solution was then heated at 318 °C with a constant heating rate of 3.3 °C min^{-1}. The reaction was allowed to proceed at this temperature for 30 min. The resulting solution containing MNPs were cooled to room temperature followed by adding 125 mL of ethanol to precipitate out the nanoparticles. The MNPs were then washed with toluene and separated by centrifugation. The synthesis of MNPs with a size of 5 nm followed similar procedures as described above. Nine grams of iron−oleate complex and 2.85 g of oleic acid were completely dissolved into 50 g of 1-octadecene at room temperature, and 8.05 g of oleyl alcohol was added into the mixture. The solution was degassed by bubbling N_2 for 15 min. Afterwards, the solution was heated at 280 °C at a constant heating rate of 10 °C min^{-1} under N_2 protection and kept at that temperature for 30 mins. Upon completion of the reaction, the nanoparticles were washed following the same steps as those for the 9 nm MNPs.

Synthesis of Random Copolymer Poly(sodium styrene-4-sulfonate)-co-poly(N-isopropylacrylamide).[46] Three grams of SSS and 17 g of NIPAM was dissolved into 115 mL of DMSO. The resulting solution was degassed by bubbling N_2 for 20 min. When the solution was heated at 80 °C, 5 mL of DMSO containing 0.92 g of ACVA was injected into the reactant solution. The reaction took 24 h to complete under the protection of a N_2 blanket. After the reaction was completed, the copolymer solution was cooled to room temperature, and acetone was added to precipitate out the copolymer. The copolymer was dried in a vacuum oven at 25 °C. On the basis of the weight percent of SSS (15%), the random copolymer PSSS-PNIPAM is denoted as 15SN. Pure poly(sodium 4-styrene sulfonate) (PSSS) and poly(*N*-isopropylacrylamide) (PNIPAM) were synthesized following the same procedures by introducing either SSS or NIPAM to the reaction. The chemical structure of the synthesized copolymer was analyzed by ^{1}H NMR spectroscopy on a Bruker Advance 500 (DRX 500 MHz) NMR spectrometer using D_2O as the solvent. The copolymer of 15SN was synthesized and analyzed with an NMR spectrometer. The ^{1}H NMR spectra of PSSS, PNIPAM, and 15SN are shown in Figure S1. The chemical shifts in the range of δ = 2.48−2.80 ppm (a) are attributable to the −CH− group linked to the phenyl moiety, whereas the chemical shift at δ = 1.06 ppm (b) is assigned to the $-CH_3$ groups in the NIPAM moieties. The chemical shift at δ = 3.81 ppm (c) can be assigned to the −CH− group adjacent to the amide group. The chemical shifts of the copolymer are consistent with those of PSSS and PNIPAM. The molecular weight of the copolymer was characterized by a Waters gel-permeation chromatography (GPC) system using DMF as the eluent at 30 °C and a flow rate of 1.0 mL min^{-1}. The average molecular weight, M_n, of the copolymer 15SN was found to be 16 270 g mol^{-1}.

Ligand Exchange. Ligand exchange was performed to replace the hydrophobic oleic acid on the surface of the MNPs with the hydrophilic 15SN. Briefly, 80 mL of toluene containing 0.4 g of MNPs was mixed with 80 mL of DMF containing 1.6 g of 15SN. The mixture was vigorously stirred with a mechanical stirrer and heated at 130 °C for 24 h. After the reaction was finished, the solution was cooled to room temperature. The resulting MNPs functionalized with the copolymer 15SN were precipitated out by adding hexane (MNP-15SN).

Characterizations. The chemical structure of the PSSS-PNIPAM copolymer was analyzed by ^{1}H NMR spectroscopy on a Bruker Advance 500 (DRX 500 MHz) NMR spectrometer using D_2O as the solvent. The molecular weight of the copolymer was characterized by gel-permeation chromatography (Waters GPC system) equipped with a Waters 1515 isocratic HPLC pump, a Waters 717 plus autosampler injector, a Waters 2414 refractive-index detector, and an Agilent PLgel 5 μm mixed-D column (no. 79911GP-MXD) using DMF as the eluent at 30 °C and a flow rate of 1.0 mL min^{-1}. The size and morphology of the MNPs were characterized by a field-emission transmission electron microscope (FETEM, JEOL JEM-2100F). Fourier-transform infrared spectroscopy (FTIR) measurements were conducted by a Bio-Rad spectrometer (FTS 3500). Functionalized magnetic nanoparticles and polymers were mixed with KBr to form pellets to determine the function groups. Thermogravimetric analysis (TGA) of the MNP-15SN, MNPs, and 15SN were performed with a thermogravimetric analyzer (Shimadzu, DTG-60AH) under N_2 from 50 to 900 °C at a temperature ramping rate of 10 °C min^{-1}. The magnetic properties of the nanoparticles were evaluated in a vibrating sample magnetometer (VSM, LakeShore 450-10) with a saturating field of 1 T at room temperature. The size change with temperature of the MNP-15SN was measured with a nanoparticle size analyzer (Nano ZS, ZEN3600).

Forward Osmosis Measurements. *Evaluation of Osmolality.* The osmolality of the MNP-15SN dispersion containing 0.5 g of MNP-15SN and 1 g of DI water was obtained using a vapor pressure osmometer (Wescor, VAPRO 5600).

Forward-Osmosis Process Using MNP-15SN as the Draw Solute. The forward-osmosis process using MNP5/MNP9-15SN as the draw solution was conducted on a lab-scale circulating-filtration unit. A commercial TFC membrane (Hydration Technologies Inc.) was used as the FO membrane. DI water, synthetic saline water (NaCl solution with a measured osmolality of 1000 mOsm kg^{-1}), and synthetic seawater (3.5 wt % NaCl solution with an osmolality of 1200 mOsm kg^{-1}) were used as feed solutions. The cross-flow membrane module consists of two rectangular channels, one on each side of the membrane, with a frame configuration of 8.0 cm in length, 1.0 cm in width, and 0.3 cm in height. The FO tests were conducted in PRO (pressure-retarded osmosis) mode with feed and draw solutions flowing concurrently at the same velocity of 15.0 cm s^{-1}. The temperatures of the feed and draw solutions were maintained at 25 ± 1 °C. Because the size of the functionalized MNPs is much larger than the pore size of the HTI FO membrane, only water is able to pass through the membrane. Therefore, any weight increase of the draw solution is only owing to water permeation from the feed solution. Because there could be a significant influence on the water permeation as a result of the concentration changes of the feed and draw solutions, the FO testing was conducted within a time period of about 1 h to avoid a large change in concentration of the draw solution. In addition, the amount of the feed solution was relatively large (>500 mL) to minimize the concentration variation. The water permeation flux, J_v (L m^{-2} h^{-1}, abbreviated as LMH), was calculated from the mass change of the feed solution as follows

$$J_v = \Delta m/(\rho A \Delta t)$$

where Δm (g) is the permeation water accumulated over a predetermined time Δt (h) during the duration of FO, A is the effective membrane surface area (m^2), and ρ is the density of water (= 1000 g L^{-1}).

Regeneration of Draw Solution and Cycling Test. After FO testing, the draw solution containing MNP-15SN was regenerated from the diluted solution. First, MNPs were separated through a high gradient magnetic separator (HGMS, S. G. Frantz Co. Inc., Isodynamic L-1) operating at 155 V and 2.4 A. The iron gauze was packed into a plastic column and fully magnetized under a magnetic field before use. When the MNP-15SN solution was introduced into the column, most of the magnetic nanoparticles were trapped in the activated iron gauze, and only small portion of MNPs and water were allowed to pass through. The gauze was demagnetized by removal of the magnetic field, and the MNPs could be easily washed out with a small amount of DI water. The filtered water with a small amount of MNPs was then subjected to ultrafiltration using a Vivaspin tube (Satrorius, Vivaspin Turbo 5K MWCO) operating at 8000 rpm for 10 min. MNPs could be separated such that only fresh water was left. All of the regenerated MNP5/MNP9-15SN could be recycled into the FO process.

■ ASSOCIATED CONTENT

Ⓢ Supporting Information

^{1}H NMR of PSSS-PNIPAM copolymer. This material is available free of charge via the Internet at http://pubs.acs.org.

■ AUTHOR INFORMATION

Corresponding Author

*E-mail: chelxm@nus.edu.sg.

Notes

The authors declare no competing financial interest.

■ ACKNOWLEDGMENTS

We are thankful for financial support from the National Research Foundation under research project R279-000-337-281. We also thank Prof. T. S. Chung and Prof. J. Y. Lee at NUS for the insightful discussions.

■ REFERENCES

(1) Elimelech, M.; Phillip, W. A. *Science* **2011**, *333*, 712−717.
(2) Cath, T. Y.; Childress, A. E.; Elimelech, M. *J. Membr. Sci.* **2006**, *281*, 70−87.
(3) Al-Obaidani, S.; Curcio, E.; Macedonio, F.; Di Profio, G.; Al-Hinai, H.; Drioli, E. *J. Membr. Sci.* **2008**, *323*, 85−98.
(4) Hu, M.; Mi, B. *Environ. Sci. Technol.* **2013**, *47*, 3715−3723.
(5) Fritzmann, C.; Löwenberg, J.; Wintgens, T.; Melin, T. *Desalination* **2007**, *216*, 1−76.
(6) Greenlee, L. F.; Lawler, D. F.; Freeman, B. D.; Marrot, B.; Moulin, P. *Water Res.* **2009**, *43*, 2317−2348.
(7) Choi, Y.-J.; Choi, J.-S.; Oh, H.-J.; Lee, S.; Yang, D. R.; Kim, J. H. *Desalination* **2009**, *247*, 239−246.
(8) Mi, B.; Elimelech, M. *Environ. Sci. Technol.* **2010**, *44*, 2022−2028.
(9) Chung, T.-S.; Zhang, S.; Wang, K. Y.; Su, J.; Ling, M. M. *Desalination* **2012**, *287*, 78−81.
(10) Liu, Z.; Bai, H.; Lee, J.; Sun, D. D. *Energy Environ. Sci.* **2011**, *4*, 2582−2585.
(11) Da Hee, J.; Lee, J.; Do Yeon, K.; Lee, Y. G.; Park, M.; Lee, S.; Yang, D. R.; Kim, J. H. *Desalination* **2011**, *277*, 83−91.
(12) Hoover, L. A.; Phillip, W. A.; Tiraferri, A.; Yip, N. Y.; Elimelech, M. *Environ. Sci. Technol.* **2011**, *45*, 9824−9830.
(13) Zhang, B.; He, Z. *RSC Adv.* **2012**, *2*, 3265−3269.
(14) Zhao, S.; Zou, L.; Tang, C. Y.; Mulcahy, D. *J. Membr. Sci.* **2012**, *396*, 1−21.
(15) Su, J.; Zhang, S.; Ling, M. M.; Chung, T.-S. *Clean Technol. Environ. Policy* **2012**, *14*, 507−511.
(16) Chan, W.-F.; Chen, H.-Y.; Surapathi, A.; Taylor, M. G.; Shao, X.; Marand, E.; Johnson, J. K. *ACS Nano* **2013**, *7*, 5308−5319.
(17) Chekli, L.; Phuntsho, S.; Shon, H. K.; Vigneswaran, S.; Kandasamy, J.; Chanan, A. *Desalin. Water Treat.* **2012**, *43*, 167−184.
(18) Ge, Q.; Ling, M.; Chung, T.-S. *J. Membr. Sci.* **2013**, *442*, 225−237.
(19) Kravath, R. E.; Davis, J. A. *Desalination* **1975**, *16*, 151−155.
(20) Kessler, J. O.; Moody, C. D. *Desalination* **1976**, *18*, 297−306.
(21) Achilli, A.; Cath, T. Y.; Childress, A. E. *J. Membr. Sci.* **2010**, *364*, 233−241.
(22) McCutcheon, J. R.; McGinnis, R. L.; Elimelech, M. *J. Membr. Sci.* **2006**, *278*, 114−123.
(23) McGinnis, R. L.; McCutcheon, J. R.; Elimelech, M. *J. Membr. Sci.* **2007**, *305*, 13−19.
(24) Phuntsho, S.; Shon, H. K.; Hong, S.; Lee, S.; Vigneswaran, S. *J. Membr. Sci.* **2011**, *375*, 172−181.
(25) Bowden, K. S.; Achilli, A.; Childress, A. E. *Bioresour. Technol.* **2012**, *122*, 207−216.
(26) Stone, M. L.; Rae, C.; Stewart, F. F.; Wilson, A. D. *Desalination* **2013**, *312*, 124−129.
(27) Ge, Q.; Su, J.; Amy, G. L.; Chung, T.-S. *Water Res.* **2012**, *46*, 1318−1326.
(28) Ge, Q.; Wang, P.; Wan, C.; Chung, T.-S. *Environ. Sci. Technol.* **2012**, *46*, 6236−6243.
(29) Yong, J. S.; Phillip, W. A.; Elimelech, M. *Ind. Eng. Chem. Res.* **2012**, *51*, 13463−13472.
(30) Ling, M. M.; Wang, K. Y.; Chung, T.-S. *Ind. Eng. Chem. Res.* **2010**, *49*, 5869−5876.
(31) Kim, Y. C.; Han, S.; Hong, S. *Water Sci. Technol.* **2011**, *64*, 469.
(32) Ling, M. M.; Chung, T.-S.; Lu, X. *Chem. Commun.* **2011**, *47*, 10788−10790.
(33) Ge, Q.; Su, J.; Chung, T.-S.; Amy, G. *Ind. Eng. Chem. Res.* **2011**, *50*, 382−388.
(34) Ling, M. M.; Chung, T.-S. *Ind. Eng. Chem. Res.* **2012**, *51*, 15463−15471.
(35) Bai, H.; Liu, Z.; Sun, D. D. *Sep. Purif. Technol.* **2011**, *81*, 392−399.
(36) Ling, M. M.; Chung, T.-S. *J. Membr. Sci.* **2011**, *372*, 201−209.
(37) Sun, G.; Chung, T.-S.; Chen, N.; Lu, X.; Zhao, Q. *RSC Adv.* **2013**, *3*, 9178−9184.
(38) Moeser, G. D.; Roach, K. A.; Green, W. H.; Alan Hatton, T.; Laibinis, P. E. *AIChE J.* **2004**, *50*, 2835−2848.

(39) Wu, J.; Gao, L.; Gao, D. *ACS Appl. Mater. Interfaces* **2012**, *4*, 3041−3046.
(40) Han, H.; Lee, J. Y.; Lu, X. *Chem. Commun.* **2013**, *49*, 6122−6124.
(41) Schild, H. G. *Prog. Polym. Sci.* **1992**, *17*, 163−249.
(42) Stuart, M. A. C.; Huck, W. T. S.; Genzer, J.; Müller, M.; Ober, C.; Stamm, M.; Sukhorukov, G. B.; Szleifer, I.; Tsukruk, V. V.; Urban, M.; et al. *Nat. Mater.* **2010**, *9*, 101−113.
(43) Noh, M.; Mok, Y.; Lee, S.; Kim, H.; Lee, S. H.; Jin, G.-W.; Seo, J.-H.; Koo, H.; Park, T. H.; Lee, Y. *Chem. Commun.* **2012**, *48*, 3845−3847.
(44) Cai, Y.; Shen, W.; Loo, S. L.; Krantz, W. B.; Wang, R.; Fane, A. G.; Hu, X. *Water Res.* **2013**, *47*, 3773−3781.
(45) Li, D.; Zhang, X.; Simon, G. P.; Wang, H. *Water Res.* **2013**, *47*, 209−215.
(46) Nowakowska, M.; Szczubiałka, K.; Gręboszc, M. *Colloid Polym. Sci.* **2004**, *283*, 291−298.
(47) Tauer, K.; Mukhamedjanova, M.; Holtze, C.; Nazaran, P.; Lee, J. *Macromol. Symp.* **2007**, *248*, 227−238.
(48) Park, J.; An, K.; Hwang, Y.; Park, J.-G.; Noh, H.-J.; Kim, J.-Y.; Park, J.-H.; Hwang, N.-M.; Hyeon, T. *Nat. Mater.* **2004**, *3*, 891−895.
(49) Neumann, O.; Urban, A. S.; Day, J.; Lal, S.; Nordlander, P.; Halas, N. J. *ACS Nano* **2013**, *7*, 42−49.
(50) Kim, B. H.; Lee, N.; Kim, H.; An, K.; Park, Y. I.; Choi, Y.; Shin, K.; Lee, Y.; Kwon, S. G.; Na, H. B.; et al. *J. Am. Chem. Soc.* **2011**, *133*, 12624−12631.